Bioorganic & Medicinal Chemistry Letters 26 (2016) 3928–3937

Contents lists available at ScienceDirect

Bioorganic & Medicinal Chemistry Letters

journal homepage: www.elsevier.com/locate/bmcl

Design and synthesis of aminothiazole modulators of the gamma-secretase enzyme

Kevin D. Rynearson [a], Ronald N. Buckle [b], Keith D. Barnes [b], R. Jason Herr [b], Nicholas J. Mayhew [b], William D. Paquette [b], Samuel A. Sakwa [b], Phuong D. Nguyen [a], Graham Johnson [c], Rudolph E. Tanzi [d], Steven L. Wagner [a,*]

[a] Department of Neurosciences, University of California, San Diego, 9500 Gilman Drive MC 0624, La Jolla, CA 92093-0624, United States
[b] Department of Medicinal Chemistry, AMRI, East Campus, 3 University Place, Rensselaer, NY 12144, United States
[c] NuPharmAdvise, 3 Lakeside Drive, Sanbornton, NH 03269, United States
[d] Genetics and Aging Research Unit, Department of Neurology, Massachusetts General Hospital, Charlestown, MA 02129, United States

ARTICLE INFO

Article history:
Received 4 May 2016
Revised 1 July 2016
Accepted 4 July 2016
Available online 6 July 2016

Keywords:
Alzheimer's disease
γ-Secretase modulators
Aminothiazoles

ABSTRACT

The design and construction of a series of novel aminothiazole-derived γ-secretase modulators is described. The incorporation of heterocyclic replacements of the terminal phenyl D-ring of lead compound **1** was conducted in order to align potency with favorable drug-like properties. γ-Secretase modulator **28** displayed good activity for in vitro inhibition of Aβ42, as well as substantial improvement in ADME and physicochemical properties, including aqueous solubility. Pharmacokinetic evaluation of compound **28** in mice revealed good brain penetration, as well as good clearance, half-life, and volume of distribution which collectively support the continued development of this class of compounds.

Alzheimer's disease (AD) is a devastating neurological disorder and is currently estimated to affect 5.3 million Americans. In 2015, AD and other related dementias will cost the United States $226 billion, and if the current disease trajectory is maintained, the associated costs could rise to as high as $1.1 trillion by 2050.[1] AD is the only top ten cause of death in America that cannot be prevented, cured or slowed, and thus there is an urgent medical need for disease modifying therapeutic agents.[1]

AD is an irreversible and progressive neurodegenerative disease affecting the brain which insidiously destroys memory, thinking skills and cognition. Originally described in 1906 by German physician Alois Alzheimer, AD is characterized by the presence of intraneuronal neurofibrillary tangles of hyperphosphorylated microtubule associated protein tau and extraneuronal neuritic plaques primarily composed of amyloid β-42 (Aβ42).[2] A large body of histopathological and genetic evidence implicates that the processing and deposition of Aβ peptides within the brain is the primary driver of AD progression ultimately leading to dementia.[3] The Aβ peptides are formed as the result of sequential proteolytic cleavages of the amyloid precursor protein (APP) by two aspartyl proteases, β-secretase (BACE-1) and γ-secretase, respectively.[4] APP is first cleaved by BACE-1 which yields membrane bound carboxy-terminal fragment-β (CTF-β) known as C99. Further cleavages of the C99 fragment by γ-secretase releases the APP intracellular domain (AICD) and produces extracellular Aβ peptides which vary in length from 37 to 43 amino acids.[5]

Directly implicated in the production of Aβ peptides, BACE-1 and γ-secretase represent attractive targets for the development of AD therapies.[3–5] Consequentially, small molecule compounds which curtail the formation of all Aβ species by inhibition of either BACE-1 or γ-secretase have been intensely pursued.[6] Potent γ-secretase inhibitors (GSI) such as semagacestat and avagacestat were developed and demonstrated robust reduction of Aβ peptides.[7] Unfortunately, these GSIs also displayed severe side effects and counter efficacy which resulted in accelerated cognitive decline during clinical evaluation, and thus γ-secretase inhibition strategies were abandoned.[8] As an alternative to inhibition, γ-secretase modulation offers an attractive approach with the goal of attenuating the production of the neurotoxic and aggregation prone Aβ42 isoform, the primary component of neuritic plaques, while not affecting endogenous γ-secretase function.[9] Based on the fact that the vast majority of the more than 200 FAD-linked genetic mutations appear to cause a 2-fold increase in the ratio of the longer Aβ42 peptide to the shorter Aβ40 peptide, and a large body of data pointing specifically to Aβ42 in pathogenesis, a therapeutic rationale that modulates γ-secretase activity to reduce the level of

* Corresponding author.
E-mail address: slwagner@ucsd.edu (S.L. Wagner).

http://dx.doi.org/10.1016/j.bmcl.2016.07.011
0960-894X/

Aβ42 relative to the shorter Aβ peptides (i.e., Aβ40, Aβ38 and Aβ37) without affecting overall γ-secretase function may prove to be an efficacious course for interrupting AD progression.[10] Several classes of γ-secretase modulators have been discovered which alter the Aβ cleavage pattern in favor of shorter Aβ peptides, including compounds derived from non-steroidal anti-inflammatory drugs (NSAIDs),[11] aryl imidazoles[5,12] and triterpenes.[13]

Previously our lab discovered a series of aminothiazole-derived γ-secretase modulators (AGSMs) through rational hit to lead optimization efforts which demonstrate remarkable potency for lowering Aβ42 (>1000-fold more potent than the NSAID-like GSM tarenflurbil) and exhibit moderate brain penetrance.[14] This novel class of compounds is characterized by a tetracyclic scaffold composed of bridged linear aromatics (Fig. 1). Compounds within this series have been shown to specifically reduce the levels of Aβ42 and Aβ40 production while simultaneously increasing the levels of Aβ38 and Aβ37, thereby leaving the total amount of Aβ produced unchanged. Importantly, AGSMs do not affect γ-secretase-mediated cleavage of other critical substrates, including Notch and E-cadherin. The selectivity for Aβ products likely stems from the observed binding of AGSMs to Pen-2 and PS-1 NTF of the γ-secretase enzymatic complex which shifts rather than inhibits endogenous function. Additionally, in vivo studies showed AGSMs were potent and effective at decreasing the levels of Aβ42 and Aβ40 in the plasma and brain of APP transgenic mice. Chronic administration of AGSMs to Tg2576 APP transgenic mice resulted in dramatic reduction of AD-like pathology in the absence of GSI-related effects such as intestinal goblet cell hyperplasia due a distinct mode of action.[14] Despite the overall efficacy of these compounds, the poor aqueous solubility (<0.1 μM at neutral pH) of the AGSMs presents a significant liability especially when attempting to achieve the supraefficacious exposures required for safety and toxicology studies during preclinical development.

Herein, we describe the development of second generation GSM compounds aimed at improving critical physicochemical properties while maintaining the potent activity of the parent AGSM. Ligand design focused on identifying heterocyclic replacements for the hydrophobic D-ring as a means to improve ADME (absorption, distribution, metabolism and excretion) parameters, as well as aqueous solubility. Replacement of the alkyl rich phenyl D-ring by a pyrazole containing scaffold was anticipated to ameliorate the property related shortcomings of the AGSMs. Based on the spatial arrangement of the substituents within AGSM **1**, as well as molecular modeling overlays, tetrahydroindazole, 3-*tert*-butylpyrazole and cyclopentapyrazole D-ring analogs were selected for preparation. The construction of the three unique series would be accomplished utilizing established Hantzsch chemistry from a common bromoacetophenone precursor enabling the rapid preparation of a diverse set of pyrazole containing scaffolds permitting rigorous evaluation of these novel D-ring substitutions (Scheme 1).[15]

A series of 3-aminotetrahydroindazole analogs were synthesized in order to explore the local spatial constraints of the γ-secretase binding cavity with respect to this novel D-ring substitution. The fused ring system of the 2-substituted tetrahydroindazole **5** was envisioned to mirror the alkyl functionalization of AGSM **1** while rigidifying the D-ring and preserving favorable hydrophobic interactions of the parent molecule. 2-Substituted tetrahydroindazoles **5**–**9** displayed modest activity for the reduction of Aβ42 in a SHSY5Y neuroblastoma cell line stably over-expressing human APP and demonstrated a slight gain in potency as the alkyl chain increases in size (compounds **5**–**7** Table 1).[16,17] However, the alteration in *N*-alkyl connectivity of tetrahydroindazole **7** providing isopropyl derivative **8**, as well as the introduction of a *tert*-butyl group in compound **9** led to a slight reduction in activity. Removal of the 2-postion substituent as illustrated by tetrahydroindazole **10** abrogates activity, underscoring the importance of the alkyl functionality with respect to Aβ modulation.

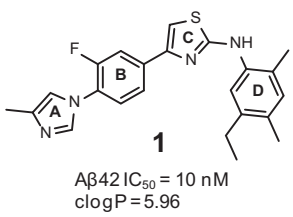

Figure 1. General scaffold of optimized lead aminothiazole-derived γ-secretase modulator (AGSM). The rings are labeled A–D for clarity.

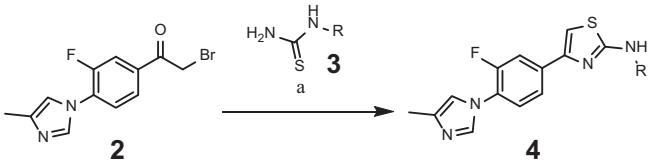

Scheme 1. Reagents and conditions: (a) EtOH, reflux, overnight, 16–79%, R = tetrahydroindazole, 3-*tert*-butylpyrazole or cyclopentapyrazole containing scaffold.

Based on the pivotal role the 2-postion substituent plays with respect activity, in addition to the overall tolerance for alkyl substituents of various size, analogs **11**–**26** were prepared to thoroughly probe the chemical space for favorable interactions. The constrained and small 2-cyclobutyl tetrahydroindazole **11** displayed a 2-fold increase in activity when compared to isopropyl analog **8**, suggesting that this region of γ-secretase features a narrow hydrophobic pocket. This assertion is further supported by ligands **12**–**16** which illustrate that as the size of the substituent increases from the 2-cyclopropyl to the larger 2-cyclohexyl derivative (**12** vs **13**) the observed activity decreases. Moreover, increasing the polarity of the 2-position substituent through the incorporation of heteroatoms as exemplified by the tetrahydrofuran **14**, tetrahydropyran **15** and 1-methylpiperidine **16** significantly erodes potency. In general, deviation from linear *N*-alkyl substitution is deleterious to suppressing Aβ42 levels, and the introduction of heteroatoms served to exacerbate this trend.

Efforts to increase the flexibility of the heterocyclic substituent, as well as extend beyond the constrained hydrophobic region through the insertion of an ethyl or propyl linker failed to restore the loss of activity as evidenced by analogs **17**, **18** and **19**. Consequentially, the incorporation of smaller functionalities within the active 2-postion alkylated analogs was explored. 2-Trifluororethane **21** demonstrated similar activity to parent analog **6**, whereas 2-fluoroethane **20** displayed a slight increase in activity for the reduction of Aβ42. The insertion of oxygen with the alkyl chain was poorly tolerated as demonstrated by 2-methoxyethane **22**, 2-hydroxyethane **23**, and 2-hydroxypropane **24** which are approximately 2-fold less active than the corresponding aliphatic analog. However, increasing hydrophobicity of analog **23** through the addition of two flanking methyl groups resulting in 2-hydroxy-2-methylpropane compound **25** showed an unexpected 3-fold improvement over primary analog **7** thus reinforcing the strong preference for hydrophobic character within this region of the D-ring by the γ-secretase enzyme. Finally, an *N*-methyl derivative of compound **26** was synthesized in order to ascertain the role of the proton with respect to ligand affinity. Unfortunately, *N*-methylated analog **26** loses all activity suggesting either the presence of a hydrogen bond between the ligand and enzyme or an overall reduction in ligand flexibility stemming from the sterical interactions between the D-ring and the added methyl which restrict access to conformations required for target interaction.

Table 1
3-Aminotetrahydroindazole D-ring analogs of AGSM **1**

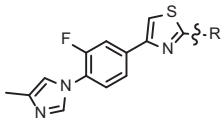

Compd	R	Aβ42 IC_{50}[a]	*c*log*P*[b]	Kinetic aqueous solubility[c]
5	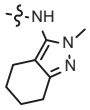	208	3.54	nt[d]
6	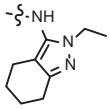	163	3.88	nt[d]
7	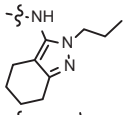	148	4.35	nt[d]
8	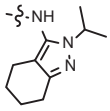	195	4.30	nt[d]
9	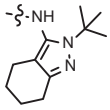	216	4.37	nt[d]
10	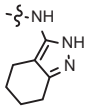	>1000	3.59	nt[d]
11	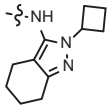	112	4.33	<1.6
12	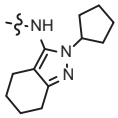	225	4.73	nt[d]
13	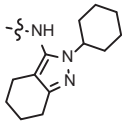	280	5.13	nt[d]
14	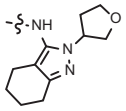	289	3.32	nt[d]
15	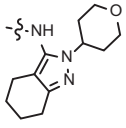	766	3.37	nt[d]
16	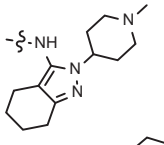	>1000	3.52	2.8
17	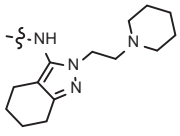	475	4.24	8.1

Table 1 (*continued*)

Compd	R	Aβ42 IC_{50}[a]	*c*log *P*[b]	Kinetic aqueous solubility[c]
18	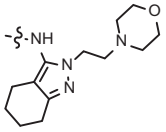	>1000	3.18	nt[d]
19	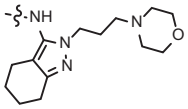	270	3.23	16
20	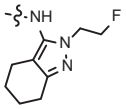	110	3.70	nt[d]
21	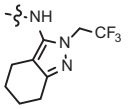	179	4.52	nt[d]
22	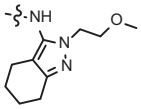	272	3.38	2.3
23	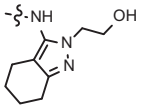	362	2.80	15
24	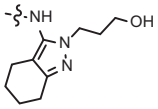	229	2.85	nt[d]
25	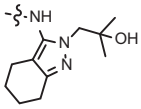	55	3.29	<1.6
26	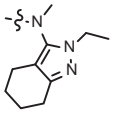	>1000	4.13	nt[d]

[a] IC_{50} represents the concentration in nM of compound required for reducing Aβ42 levels by 50%. The IC_{50} values are the mean of at least 2 determinations.[16,17]

[b] Calculated partition coefficient of the ratio of the compound's concentration in octanol to the compound's concentration in water using ChemAxon.

[c] Kinetic solubility measured at pH 7.4 by UV/Vis absorbance in PBS buffer (μM).

[d] nt = not tested—compound did not meet minimum activity threshold (Aβ42 $IC_{50} \leqslant 100$ nM).

Optimization of the tetrahydroindazole series led to the discovery of two moderately potent γ-secretase modulators, 2-cyclobutane **11** and 2-hydroxy-2-methylpropane **25** which were subsequently evaluated in a kinetic aqueous solubility assay. Unfortunately, neither analog demonstrated improved solubility (Table 1). However, the incorporation of heteroatoms within the D-ring does lead to compounds which exhibit ideal solubility as demonstrated by analogs **17**, **19** and **23**, albeit at the expense of modulator activity. Modest improvements in aqueous solubility were also observed for 1-methylpiperidine **16** and 2-methoxyethane **22**, thus validating our synthetic strategy for addressing this property related shortcoming. In addition, integrating heteroatoms within the 2-position substituent of the tetrahydroindazole family of compounds was found to result in ligands with poor microsomal stability (data not shown). Thus, our efforts to maintain activity for inhibiting the formation of Aβ42 while improving ligand solubility through the introduction of novel tetrahydroindazole D-ring scaffolds provided ligands with fair activity, but lacking the desired physicochemical properties of a drug-like compound. Therefore, additional analogs were explored which retain the pyrazole core of this series to determine the effect of the fused ring system on ligand activity, as well as on aqueous solubility.

In order to improve upon the tetrahydroindazole family of compounds, as well as further enhance our understanding of D-ring interactions with the γ-secretase enzyme, a novel set of 1-substituted 3-*tert*-butylpyrazole ligands was designed and synthesized with the goal of simultaneously increasing potency and improving aqueous solubility. The placement of substituents was again modeled on preserving favorable hydrophobic interactions present in the D-ring of AGSM **1**. Additionally, the *tert*-butyl substitution was envisaged to allow the exploration of new regions within the target through the use of a bulky substituent directed into a specific region of space while simultaneously increasing overall ligand flexibility when compared to its fused ring counterpart. Alkylated pyrazole analogs **27**–**31** were prepared based on the moderate Aβ42 reduction observed in the 2-substituted tetrahydroindazole series (Table 2). The novel 1,3-disubstitiuted pyrazole compounds displayed modest to good activity, with *N*-ethyl derivative **28** displaying the best Aβ42-lowering activity with an IC_{50} = 63 nM. The incorporation of longer alkyl chains did not lead

Table 2
1-Substituted 3-*tert*-butylpyrazole D-ring analogs of AGSM **1**

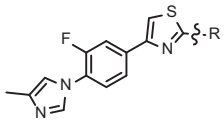

Compd	R	Aβ42 IC_{50}[a]	*c*log*P*[b]	Kinetic aqueous solubility[c]
27	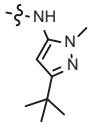	294	4.41	nt[d]
28	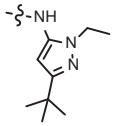	63	4.75	4.7
29	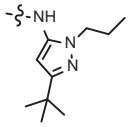	86	5.22	<1.6
30	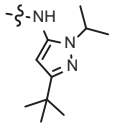	87	5.16	5.5
31	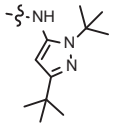	85	5.24	2.0
32	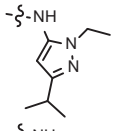	394	4.09	nt[d]
33	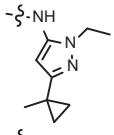	67	4.25	<1.6
34	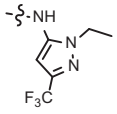	110	4.01	<1.6
35	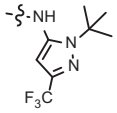	121	4.50	nt[d]
36	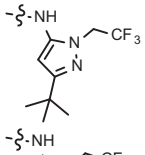	87	5.38	<1.6
37	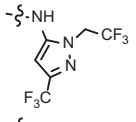	771	4.64	nt[d]
38	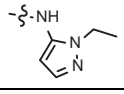	>1000	2.72	nt[d]

[a] IC_{50} represents the concentration in nM of compound required for reducing Aβ42 levels by 50%. The IC_{50} values are the mean of at least 2 determinations.[16,17]
[b] Calculated partition coefficient of the ratio of the compound's concentration in octanol to the compound's concentration in water using ChemAxon.
[c] Kinetic solubility measured at pH 7.4 by UV/Vis absorbance in PBS buffer (μM).
[d] nt = not tested—compound did not meet minimum activity threshold (Aβ42 $IC_{50} \leqslant 100$ nM).

to improved potency as observed with the tetrahydroindazoles. Also distinct, the larger *N*-isopropyl analog **30** and *N*-*tert*butyl analog **31** did not adversely impact the potency of this series. The improved activity of compounds **28**–**31** was also accompanied by a modest improvement in aqueous solubility; pyrazoles **28**, **30** and **31** displayed improved solubility, while compound **29** maintained the poor solubility associated with many of the ligands developed thus far.

The initially prepared 1-substituted 3-*tert*-butylpyrazole ligands (**28**–**31**) demonstrated consistent potency over a wide range of alkyl substitutions. The improved properties of the 3-*tert*-butylpyrazole set of ligands led us to explore additional analogs of *N*-ethyl pyrazole **28**. Ligand design focused on potential modifications to the pyrazole substitution pattern which probe the subtle interactions between the compound and the target. Introduction of a 3-isopropyl substituent (**32**) within the pyrazole resulted in a 6-fold reduction in activity when compared to compound **28** (Table 2). On the other hand, 3-methylcyclopropyl **33** maintained potency, suggesting the overall hydrophobic bulk within the 3-position of the pyrazole is relevant to binding affinity. Surprisingly, the integration of a smaller 3-trifluoromethyl substituent in pyrazole **34** was tolerated. In addition, similar to the loss in potency observed between 3-*tert*-butylpyrazoles **28** and **31**, *N*-*tert*butyl-3-trifluoromethyl analog **35** only showed a minor loss in activity associated with the larger amino substituent. The preservation of activity associated with the 3-trifluoromethyl analogs **34** and **35** is hypothesized to result from the maintained favorable hydrophobic interactions of the *N*-substituent within the enzyme target, as well as a substantial reduction in the penalty associated with the lost interactions of the 3-*tert*butyl substituent through unanticipated electronic effects of the trifluoromethyl replacement. The incorporation of *N*-trifluoroethyl was also explored resulting in derivative **36** which showed comparable activity to 3-trifluoromethyl pyrazole **34**. However, *N*-trifluoroethyl-3-trifluoromethyl pyrazole **37** displays a greater than 10-fold loss in activity lending support to the notion that the presence of a hydrophobic substituent within the D-ring is required in order to maintain ligand affinity. Furthermore, the removal of the 3-position substituent as illustrated by *N*-ethylpyrazole analog **38** results in a complete loss of activity for the suppression of Aβ42 formation.

The focused set of additional pyrazole analogs allowed the identification of three additional moderately potent γ-secretase modulators, **33**, **34** and **36** which were subsequently screened in a kinetic solubility assay. Unfortunately, neither the architectural changes in analog **33** nor the integration of trifluoro substituents in analogs **34** and **36** resulted in an increase in solubility despite the decrease in the *c*log*P* observed for compounds **33** and **34**. Even though few ligands within the series showed improved solubility, overall the prepared *tert*butylpyrazole family of compounds provided tremendous insight into the specific interactions within the D-ring which govern biological potency.

As a complement to the tetrahydroindazoles and the substituted *tert*-butylpyrazoles, a novel set of compounds containing a cyclopentapyrazole D-ring were also explored. The primary design objective within this series was to evaluate whether contraction of the fused ring system would mitigate potential unfavorable clashes within the binding cleft resulting from the larger tetrahydroindazole scaffold while reducing the overall hydrophobic character of the substituent thereby improving aqueous solubility. Additionally, the substituted cyclopentapyrazoles were envisaged to broaden the structure-activity relationship (SAR) data through the incorporation of structural features which conferred activity to the previously prepared analogs within the context of this distinct scaffold.

Cyclopentapyrazole analogs **39**–**45** were synthesized based on the most active compounds within the tetrahydroindazole series. *N*-Methyl derivative **39** was unexpectedly inactive toward reducing the generation of Aβ42. However, *N*-ethylcyclopentapyrazole **40**, *N*-isopropylcyclopentapyrazole **41** and *N*-trifluoroethylcyclopentapyrazole **44** displayed good potency and were 4-fold, 3-fold and 2-fold superior to the corresponding tetrahydroindazoles **6**, **8** and **21**, respectively. However, *N*-*tert*-butyl compound **42** and *N*-cyclobutyl compound **43** were unaffected by the contraction of the fused ring system and displayed commensurate activity to the analogous tetrahydroindazoles **9** and **11**, respectively. Efforts to incorporate a more polar amino substituent resulted in

Table 3
1-Substituted 3-*tert*-butylpyrazole D-ring analogs of AGSM **1**

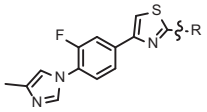

Compd	R	Aβ42 IC_{50}[a]	*c*log*P*[b]	Kinetic aqueous solubility[c]
39	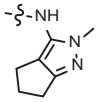	>1000	3.14	nt[d]
40	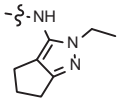	41	3.49	<1.6
41	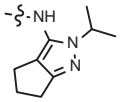	66	3.90	<1.6
42	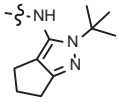	175	3.98	nt[d]
43	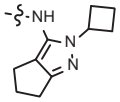	92	3.94	<1.6
44	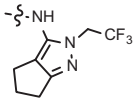	94	4.12	<1.6
45	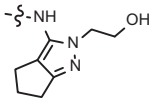	>1000	2.40	<1.6
46	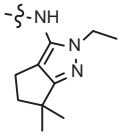	62	4.71	2.1
47	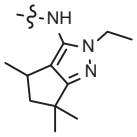	49	5.04	2.6
48	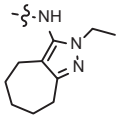	114	4.28	nt[d]

[a] IC_{50} represents the concentration in nM of compound required for reducing Aβ42 levels by 50%. The IC_{50} values are the mean of at least 2 determinations.[16,17]
[b] Calculated partition coefficient of the ratio of the compound's concentration in octanol to the compound's concentration in water using ChemAxon.
[c] Kinetic solubility measured at pH 7.4 by UV/Vis absorbance in PBS buffer (μM).
[d] nt = not tested—compound did not meet minimum activity threshold (Aβ42 $IC_{50} \leqslant 100$ nM).

a complete loss of activity as evidenced by *N*-hydroxyethyl analog **45**. The absence of a general tendency toward improved activity indicates that the smaller D-ring is not solely responsible for improved potency of the cyclopentapyrazole series. Additionally, increasing the size of the fused ring system to the corresponding cycloheptapyrazole, **48**, provides an analog with activity superior to the analogous tetrahydroindazole **6**, demonstrating the absence of a direct connection between size and activity within this particular region of the D-ring. Thus, the specific interactions of the non-planar fused D-ring system, as well as the alkyl amino substituent are crucial to facilitating favorable interactions within this region of the γ-secretase enzyme.

In order to correlate the binding mode of the substituted *tert*-butylpyrazoles within the cyclopentapyrazole family of compounds, 6,6-dimethylcyclopentapyrazole analogs **46** and **47** were also synthesized. The dimethyl substituent of compound **46** was anticipated to occupy the hydrophobic region of γ-secretase in a similar fashion to *tert*-butyl group of pyrazole **28**, however within the context of a more rigid scaffold. In addition, the slightly larger trimethylcyclopentapyrazole **47** was conceived to explore the breadth of the binding pocket. Surprisingly, both ligands maintained similar activity to the parent pyrazole **40**, displaying IC_{50} values of 62 nM and 49 nM for the inhibition of Aβ42, respectively. The unanticipated activity of both ligands demonstrates that there is little to no penalty associated with incorporation of methyl substituents at either the 4- or 6-positions of cyclopentapyrazole signifying the presence of a wide cavity which may yield, upon further exploration, favorable interactions with less hydrophobic moieties.

The focused set of cyclopentapyrazoles produced six compounds with sufficient activity to warrant the evaluation of kinetic solubility. Despite the improved activity of the series, these compounds remain stalwartly insoluble (Table 3), indicating the need for additional chemical modifications which address aqueous solubility. However, the general tendency of adding of more hydrophobic bulk to the D-ring in order to produce compounds with the desired activity runs counter to the overarching goal of increasing solubility and improving other related physicochemical properties. Therefore, D-ring optimization may not be an ideal avenue to address the underlying property related issues of the cyclopentapyrazole scaffold.

Chemical optimization of AGSM **1** through the construction of three related D-ring series of compounds led to the discovery of various novel ligands with good activity for suppressing the formation of Aβ42 through modulating the activity of the γ-secretase enzyme. Unfortunately, many of the ligands identified suffered from poor aqueous solubility. However, a subset of the ligands within the 1-substituted 3-*tert*-butylpyrazoles series displayed both good activity, as well as improved aqueous solubility. The most potent compound discovered within the series, *N*-ethylpyrazole **28**, displayed good potency for suppressing Aβ42 with an IC_{50} value of 63 nM, in addition to moderate solubility (Table 4). Consequentially, further in vitro ADMET (Absorption, Distribution, Metabolism, Excretion and Toxicology) analysis of *N*-ethylpyrazole **28** was undertaken in order to identify potential liabilities within this family of compounds which would preclude further development. *N*-Ethylpyrazole **28** demonstrated ideal CyP inhibition potential and hERG ion channel inhibition potential (all IC_{50} values >10 μM). In addition, compound **28** showed fair microsomal stability. However, poor membrane permeability as measured by MDR1-MDCK assay and high plasma protein binding were also observed for *N*-ethylpyrazole **28**. Despite the limited in vitro membrane permeability, compound **28** was selected for in vivo pharmacokinetic (PK) studies in order to gauge critical PK parameters, determine whether this ligand can reach the intended enzyme target within the brain and establish a baseline for future compound development with respect to SAR/SPR.

Table 4
In vitro ADMET properties of pyrazole **28**

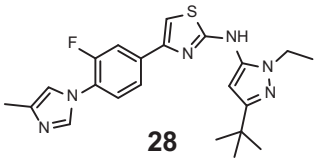

28

Aβ42 IC_{50} (nM)	63
Kin. sol. pH 7.4 (μM)[a]	4.7
*c*log*P*	4.75
log*D*	3.64
hLM (%)[b]	51
rLM (%)[b]	64
mLM (%)[b]	95
CYP450 IC_{50} (μM)[c]	
3A4	16
1A2	>100
2C9	>100
2C19	82
2D6	>100
hERG IC_{50} (μM)[d]	>30
P_{app}[e]	0.97
Efflux ratio[f]	1.6
% PPB[g]	99.4

[a] Kinetic solubility measured at pH 7.4 by UV/Vis absorbance in PBS buffer (μM).
[b] % remaining after 30 min upon incubation with human (hLM), rat (rLM) and mouse (mLM) liver microsomes (1 mg/mL), at 1 μM test compound concentration.
[c] Five recombinant CYP isoforms were tested for inhibition by the test compound using fluorescence-based assays.
[d] Patch-Xpress patch-clamp assay; compounds were tested ($n = 3$) in a five-point concentration–response on HEK-293 cells stably expressing the hERG channel.
[e] Apparent permeability (A–B; $\times 10^{-6}$ cm/s) determined in MDR1-MDCK cell monolayers.
[f] Calculated efflux ratio determined using MDR1-MDCK cell monolayers (B–A/A–B).
[g] % PPB = plasma protein binding.

Table 5
Mouse in vivo pharmacokinetic study of pyrazole **28**

	iv	po
Mouse pharmacokinetics of **28**[a]		
Dose (mg/kg)	1	5
C_{max} (ng/mL)	161	1005
T_{max} (h)	0.083	1.0
$t_{1/2}$ (h)	2.4	6.0
AUC_{last} (ng·h/mL)	335	5393
AUC_{inf} (ng·h/mL)	498	5720
Cl (mL/h/kg)	2009	
V_{SS} (mL/kg)	7152	
F (%)	100	>100
Brain/plasma ratio (@ 1 h post dose)	0.64	0.50
Brain/plasma ratio (@ 4 h post dose)	nc[b]	0.53
Brain/plasma ratio (@ 8 h post dose)	nc[b]	0.59

[a] CD-1 male mice $n = 24$.
[b] Not collected.

As shown in Table 5, in vivo dosing of *N*-ethylpyrazole **28** in male CD-1 mice revealed that kinetically compound **28** has a relatively high clearance (CL) and a short plasma half-life ($t_{½}$), despite the high metabolic stability observed in the in vitro mouse microsomal stability assay.[18] Following IV administration at 1 mg/kg in mice, the clearance of compound **28** was 2009 mL/hr/kg (or 33.5 mL/min/kg) which is about 40% of mouse hepatic blood flow (~80 mL/min/kg), while its half-life ($t_{½}$) was 2.4 h. Although compound **28** has a relatively large volume of distribution (V_{ss} = 7.15 L/kg), which is about 11-fold higher than body water (~0.65 L/kg), it has a short half-life due mainly to its high rate of clearance. The bioavailability (*F*) of *N*-ethylpyrazole **28** is unexpectedly high and is estimated to be 230%.

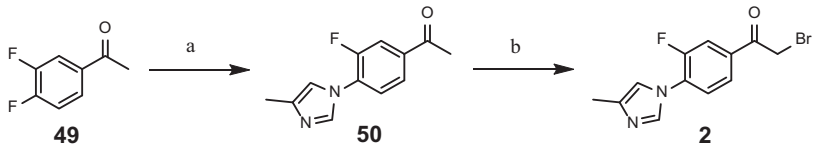

Scheme 2. Reagents and conditions: (a) 4-Methyl-1*H*-imidazole, K_2CO_3, DMSO, 55 °C, overnight, 58%; (b) Br_2, $CHCl_3$, 30% HBr in acetic acid, rt, 3 h, 100%.

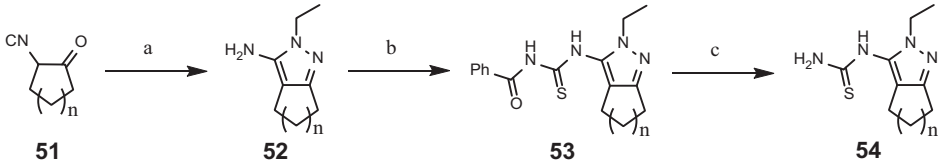

Scheme 3. For substrates n = 1 or 2. Reagents and conditions: (a) Ethylhydrazine oxalate, EtOH, reflux, overnight, 45%; (b) benzoyl isothiocyanate, 60 °C, 3.5 h, 99%; (c) K_2CO_3, MeOH, THF, rt, overnight, 90%.

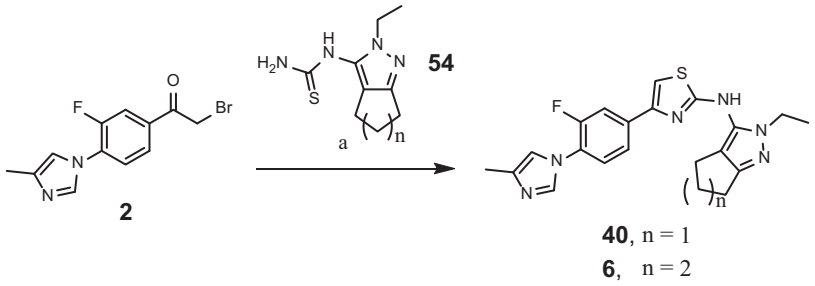

Scheme 4. Reagents and conditions: (a) EtOH, reflux, overnight, n = 1, 78%, n = 2, 24%.

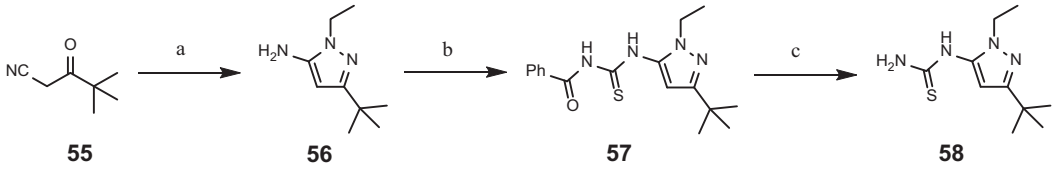

Scheme 5. Reagents and conditions: (a) Ethylhydrazine oxalate, EtOH, reflux, overnight, 61%; (b) benzoyl isothiocyanate, acetone, reflux, 3.5 h, 88%; (c) K_2CO_3, MeOH, THF, rt, overnight, 92%.

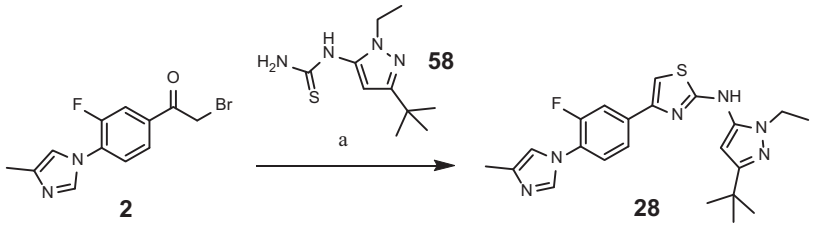

Scheme 6. Reagents and conditions: (a) EtOH, reflux, overnight, 23%.

Theoretically, the bioavailability should not exceed 100%, and one would expect based on the clearance of compound **28** being 40% of mouse hepatic blood flow that significant hepatic first-pass metabolism would result in bioavailability much less than 100%, even when the compound is completely absorbed from the intestinal lumen. The high bioavailability is hypothesized to be the result of saturation of hepatic drug metabolism during oral absorption. Following the oral dose of 5 mg/kg, the concentration of *N*-ethylpyrazole **28** is very high in the portal vein which saturates the drug metabolizing enzymes in the liver and results in decreased compound clearance leading to a marked increase in the oral AUC and an over estimation of *F*. *N*-Ethylpyrazole **28** also shows good brain penetrance for both routes of administration, in contrast to the in vitro permeability assay results. Kinetically, the mouse PK parameters (CL, $t_{½}$ and V_{ss}) of compound **28** are reasonably good and support further development efforts surrounding this class of compounds.

In order to facilitate the preparation of 2-aminothiazoles containing novel D-ring substitutions, a convergent synthetic route was selected which requires the synthesis of common precursor

2. Straightforward aromatic substitution of 3,4-difluoroacetophenone using 4-methylimidazole provided access to 2-imidazolylacetophenone intermediate **50** in fair yield (Scheme 2).[19] Subsequent acid-catalyzed bromination allowed isolation of the desired bromoacetophenone compound **2** in quantitative yield.[20] The construction of the complementary cyclopentapyrazole fragment toward the synthesis of 2-aminothiazole **40** commenced with the condensation of 2-cyanocyclopentanone with ethylhydrazine in order to afford 3-aminocyclopentapyrazole **52** (Scheme 3).[21] Subsequent reaction of intermediate **52** with benzoyl isothiocyanate furnished benzoyl thiourea **53** in good yield. Isolation of the desired cyclopentapyrazole coupling partner **54** was accomplished following removal of the benzoyl group using K_2CO_3. Assembly of the desired final product was then accomplished by Hantzsch condensation of thiourea **54** with bromoethanone **2** to afford aminothiazole **40** in good yield (Scheme 4). This general approach provided access to tetrahydroindazoles **5**–**26**, as well as cyclopentapyrazoles **39**–**48** by selecting the appropriate starting material and utilizing an assortment of commercially available substituted hydrazines in the synthetic sequence.

A similar synthetic sequence was utilized to isolate the 3-*tert*-butylpyrazole series of γ-secretase modulators. The condensation of ethylhydrazine with 4,4-dimethyl-3-oxopentanenitrile furnished substituted aminopyrazole **56** (Scheme 5).[21] The subsequent reaction of intermediate **56** with benzoyl isothiocyanate followed by base mediated removal of the benzoyl protecting group provided the desired coupling partner, pyrazolylthiourea **58**, in good overall yield. Finally, reaction between intermediate **58** and common precursor **2** gave the desired aminothiazole **28** (Scheme 6). The use of a convergent synthetic strategy provided access to a large assortment of novel D-ring ligands enabling rapid evaluation of structure–activity relationships within the three related series.

In summary, using poorly soluble AGSM **1** as the starting point, a novel series of γ-secretase modulator D-ring analogs possessing a common pyrazole moiety were synthesized leading to the discovery of compounds from three unique families which demonstrate moderate activity for suppressing the formation of Aβ42. Unfortunately, the heterocyclic D-ring derivatives did not provide the anticipated broad increase in compound solubility. Furthermore, the SAR indicated an overall trend in which increasing the lipophilicity of the D-ring leads to improved activity and consequentially reduced aqueous solubility, as well as less than stellar drug-like properties. Despite these challenges, ligands within the 1-substituted 3-*tert*-butylpyrazole series displayed reasonably good activity and substantially improved properties including aqueous solubility. Rigorous ADME evaluation of the most potent molecule within the family, *N*-ethylpyrazole **28**, revealed an overall good profile with the exception of poor membrane permeability and high plasma protein binding. However, the reasonably good in vivo PK behavior exhibited by pyrazole **28** indicates the need for further development of this scaffold aimed at improving potency, as well as crucial ADME parameters including membrane permeability and aqueous solubility. Based on literature analysis, modulator design has now shifted toward novel B-ring analogs in order to address continuing property related issues and these efforts will be reported in due course.[22]

Funding sources: This work was supported by grants from the Cure Alzheimer's Fund; and the National Institutes of Health Grant U01-NS074501.

Acknowledgments

The authors would like to thank Jiunn H. Lin of Biopharm Consulting Partners for his contribution to the in vivo pharmacokinetic studies.

Supplementary data

Supplementary data associated with this article can be found, in the online version, at http://dx.doi.org/10.1016/j.bmcl.2016.07.011.

References and notes

1. Alzheimer's Association *Alzheimer's Demen.* **2015**, *11*, 332.
2. (a) Glenner, G. G.; Wong, C. W. *Biochem. Biophys. Res. Commun.* **1984**, *120*, 885; (b) Masters, C. L.; Simms, G.; Weinman, N. A.; Multhaup, G.; McDonald, B. L.; Beyreuther, K. *Proc. Natl. Acad. Sci. U.S.A.* **1985**, *82*, 4245; (c) Iwatsubo, T.; Saido, T. C.; Mann, D. M.; Lee, V. M.; Trojanowski, J. Q. *Am. J. Pathol.* **1996**, *149*, 1823; (d) Dickson, D. W. *J. Neuropathol. Exp. Neurol.* **1997**, *56*, 321; (e) Liao, L.; Cheng, D.; Wang, J.; Duong, D. M.; Losik, T. G.; Gearing, M.; Rees, H. D.; Lah, J. J.; Levey, A. I.; Peng, J. *J. Biol. Chem.* **2004**, *279*, 37061.
3. (a) Hardy, J.; Selkoe, D. J. *Science* **2002**, *297*, 353; (b) Tanzi, R. E.; Bertram, L. *Cell* **2005**, *120*, 545.
4. (a) Thinakaran, G.; Koo, E. H. *J. Biol. Chem.* **2008**, *283*, 29615; (b) De Strooper, B.; Vassar, R.; Golde, T. *Nat. Rev. Neurol.* **2010**, *6*, 99; (c) Karrran, E.; Mercken, M.; De Strooper, B. *Nat. Rev. Drug Disc.* **2011**, *10*, 698.
5. (a) Oehlrich, D.; Berthelot, D. J.; Gijsen, H. J. M. *J. Med. Chem.* **2011**, *54*, 669; (b) Evin, G.; Barakat, A.; Masters, C. L. *Int. J. Biochem. Cell Biol.* **2010**, *42*, 1923.
6. (a) Durham, T. B.; Shepherd, T. A. *Curr. Opin. Drug Disc. Devel.* **2006**, *9*, 776; (b) Stachel, S. J. *Drug Dev. Res.* **2009**, *70*, 101; (c) Vassar, R.; Kandalepas, P. C. *Alzheimer's Res. Ther.* **2011**, *3*, 20.
7. Bateman, R. J.; Siemers, E. R.; Mawuenyega, K. G.; Wen, G.; Browning, K. R.; Sigurdson, W. C.; Yarasheski, K. E.; Friedrich, S. W.; DeMattos, R. B.; May, P. C.; Paul, S. M.; Holtzman, D. M. *Ann. Neurol.* **2009**, *66*, 48.
8. (a) Tomita, T. *Exp. Rev. Neurother.* **2009**, *9*, 661; (b) Imbimbo, B. P.; Panza, F.; Frisardi, V.; Solfrizzi, V.; D'Onofrio, G.; Logroscino, G.; Seripa, D.; Pilotto, A. *Expert Opin. Investig. Drugs* **2011**, *20*, 325.
9. (a) Van Broeck, B.; Chen, J. M.; Trenton, G.; Desmidt, M.; Hopf, C.; Ramsden, N.; Karran, E.; Mercken, M.; Rowley, A. *Br. J. Pharmacol.* **2011**, *163*, 375; (b) Wagner, S. L.; Tanzi, R. E.; Mobley, W. C.; Galasko, D. *Arch. Neurol.* **2012**, *69*, 1255.
10. (a) Iwatsubo, T.; Odaka, A.; Suzuki, N.; Mizusawa, H.; Nukina, N.; Ihara, Y. *Neuron* **1994**, *13*, 45; (b) Weggen, S.; Erikson, J. L.; Das, P.; Sagi, S. A.; Wang, R.; Pietrzik, C. U.; Findlay, K. A.; Smith, T. E.; Murphy, M. P.; Butler, T.; Kang, D. E.; Marquez-Sterling, N.; Golde, T. E.; Koo, E. H. *Nature* **2001**, *414*, 212; (c) Kumar-Singh, S.; Theuns, J.; Van Broek, B.; Pirici, D.; Vennekens, K.; Corsmit, E.; Cruts, M.; Dermaut, B.; Wang, R.; Van Broeckhoven, C. *Hum. Mutat.* **2006**, *27*, 686; (d) Rynearson, K. D.; Tanzi, R. E.; Wagner, S. L. In *Translation Neuroscience: Fundamental Approaches for Neurological Disorders*; Tuszynski, M. H., Ed.; Springer Science: New York, 2016; pp 359–368.
11. (a) Bulic, B.; Ness, J.; Hahn, S.; Rennhack, A.; Jumpertz, T.; Weggen, S. *Curr. Neuropharmacol.* **2011**, *9*, 598; (b) Jumpertz, T.; Rennhack, A.; Ness, J.; Baches, S.; Pietrzik, C. U.; Bulic, B.; Weggen, S. *PLoS One* **2012**, *7*, e30484.
12. (a) Wan, Z.; Hall, A.; Jin, Y.; Xiang, J. N.; Yang, E.; Eatherton, A.; Smith, B.; Yang, G.; Yu, H.; Wang, J.; Ye, L.; Lau, L. F.; Yang, T.; Mitchell, W.; Cai, W.; Zhang, X.; Sang, Y.; Wang, Y.; Tong, Z.; Cheng, Z.; Hussain, I.; Elliot, J. D.; Matsuoka, Y. *Bioorg. Med. Chem. Lett.* **2011**, *21*, 4016; (b) Velter, A. I.; Bischoff, F. P.; Berthelot, D.; De Cleyn, M.; Oehlrich, D.; Jaroskova, L.; Macdonald, G.; Minne, G.; Pieters, S.; Rombouts, F.; Van Brandt, S.; Van Roosbroeck, Y.; Surkyn, M.; Trabanco, A. A.; Tresadern, G.; Wu, T.; Borghys, H.; Mercken, M.; Masungi, C.; Gijsen, H. *Bioorg. Med. Chem. Lett.* **2014**, *24*, 5805; (c) Pettersson, M.; Johnson, D. S.; Humphery, J. M.; am Ende, C. W.; Evrard, E.; Efremov, I.; Kauffman, G. W.; Stepan, A. F.; Stiff, C. M.; Xie, L.; Bales, K. R.; Hajos-Korcsok, E.; Murrey, H. E.; Pustilnik, L. R.; Steyn, S. J.; Wood, K. M.; Verhoest, P. R. *Bioorg. Med. Chem. Lett.* **2015**, *25*, 908.
13. (a) Findeis, M. A.; Schroeder, F.; McKee, T. D.; Yager, D.; Fraering, P. C.; Creaser, S. P.; Austin, W. F.; Clardy, J.; Wang, R.; Selkoe, D.; Eckman, C. B. *ACS Chem. Neurosci.* **2012**, *3*, 941; (b) Fuller, N. O.; Hubbs, J. L.; Austin, W. F.; Creaser, S. P.; McKee, T. D.; Loureiro, R. M. B.; Tate, B.; Xia, W.; Ives, J. L.; Findeis, M. A.; Bronk, B. S. *ACS Med. Chem. Lett.* **2012**, *3*, 908.
14. Kounnas, M. Z.; Danks, A. M.; Cheng, S.; Tyree, C.; Mao, L.; Comer, D.; Yu, C.; Pleynet, D.; Nyugen, P.; Digregorio, P. J.; Page, N.; Ackerman, E.; Velicelebi, G.; Stauderman, K. A.; Sisodia, S. S.; Comer, W. T.; Tanzi, R. E.; Wagner, S. L. *Neuron* **2010**, *67*, 769.
15. (a) Hantzsch, A. *Ber. Dtsch. Chem. Ges.* **1881**, *14*, 1637; (b) Hantzsch, A. *Ann. Chem.* **1892**, 1.
16. Wagner, S. L.; Zhang, C.; Cheng, S.; Nguyen, P.; Zhang, X.; Rynearson, K. D.; Wang, R.; Sisodia, S. S.; Mobley, W. C.; Tanzi, R. E. *Biochemistry* **2014**, *53*, 702.
17. Aβ42 levels were quantified in human SHSY5Y neuroblastoma cells stably over-expressing human APP751 following treatment for 24 h with either vehicle or compound. The quantity of Aβ42 was then measured by ELISA, see Supplemental information for additional experimental details.
18. Male CD-1 mice were administered a single dose of vehicle, 1 mg/kg GSM **28** by IV or 5 mg/kg GSM **28** by oral gavage. Brain and plasma samples were collected at 1 h, 4 h, 8 h and 24 h post-dose. See Supplemental information for additional experimental details.
19. Wagner, S. L.; Cheng, S.; Mobley, W. C.; Tanzi, R. E. U.S. Patent US20130165416 A1, 2013.
20. (a) Möhlau, R. *Ber. Dtsch. Chem. Ges.* **1882**, *15*, 2464; (b) Hanifin, J. W.; Johnson, B. D.; Menschik, J.; Ridge, D. N.; Sloboda, A. E. *J. Pharm. Sci.* **1979**, *68*, 535; (c)

Ridge, D. N.; Hanifin, J. W.; Harten, L. A.; Johnson, B. D.; Menschik, J.; Nicolau, G.; Sloboda, A. E.; Watts, D. E. *J. Med. Chem.* **1979**, *22*, 1385.
21. (a) Taylor, E. C.; Barton, J. W. *J. Am. Chem. Soc.* **1959**, *81*, 2448; (b) Adachi, I.; Yamamori, T.; Hiramatsu, Y.; Sakai, K.; Sato, H.; Kawakami, M.; Uno, O.; Udea, M. *Chem. Pharm. Bull.* **1986**, *35*, 3235.
22. (a) Portelius, E.; Van Broeck, B.; Andreasson, U.; Gustavsson, M. K.; Mercken, M.; Zetterberg, H.; Borghys, H.; Blennow, K. *J. Alzheimer's Dis.* **2010**, *21*, 1005; (b) Nakano-Ito, K.; Fujikawa, Y.; Hihara, T.; Shinjo, H.; Kotani, S.; Suganuma, A.; Aoki, T.; Tsukidate, K. *Toxicol. Sci.* **2013**, *137*, 249.